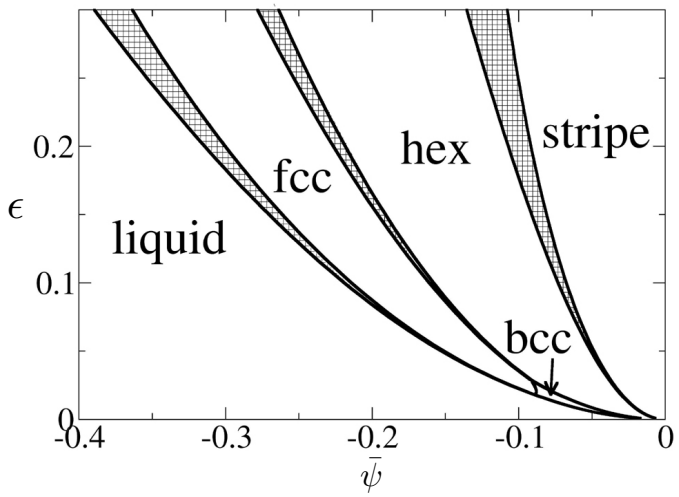

FIG. 1: Phase diagram of the two-mode PFC model for $R_1 = 0.05$ computed using two-mode and one-mode expansions of the crystal density field for fcc and bcc, respectively.

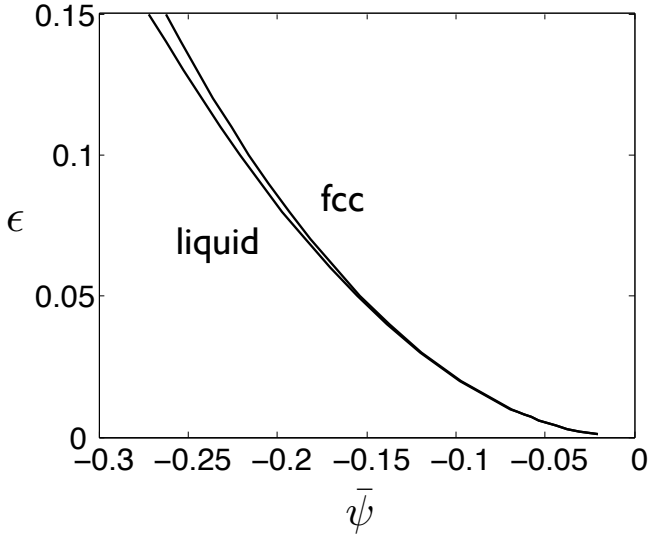

FIG. 2: Phase diagram of the two-mode PFC model showing only the fcc-solidus and liquidus for the case $R_1 = 0$ where fcc-liquid coexistence extends to vanishingly small ϵ.

B. Phase diagram

The phase diagram of the two-mode PFC model is obtained by computing the free-energy density as a function of the mean density $\bar{\psi}$ in solid and liquid, denoted by $f_s(\bar{\psi})$, and $f_l(\bar{\psi})$, respectively, and then using a standard common tangent construction to obtain equilibrium values of $\bar{\psi}$ in solid ($\bar{\psi}_s$) and liquid ($\bar{\psi}_l$).

Since the density is constant in the liquid, f_l is obtained directly from Eq. (20)

$$f_l(\bar{\psi}_l) = -(\epsilon - \frac{16}{9} - R_1)\frac{\bar{\psi}_l^2}{2} + \frac{\bar{\psi}_l^4}{4}. \qquad (26)$$

For small ϵ, the solid free-energy density can be well approximated by only considering the contribution of the $\langle 111\rangle$ and $\langle 200\rangle$ RLVs. Accordingly, the crystal density field is expanded in the form

$$\begin{aligned}\psi(\vec{r}) &\approx \bar{\psi} + \sum_{\vec{K}_i=\langle 111\rangle} A_i\, e^{i\vec{K}_i\cdot\vec{r}} + \sum_{\vec{K_j}'=\langle 200\rangle} B_j\, e^{i\vec{K_j}'\cdot\vec{r}} \\ &\approx \bar{\psi} + 8A_s\cos qx\cos qy\cos qz \\ &\quad +2B_s(\cos 2qx + \cos 2qy + \cos 2qz), \qquad (27)\end{aligned}$$

where we have used the fact that all density waves have the same amplitude in the crystal ($|A_i| = A_s$ and $|B_i| = B_s$) and the magnitude of the principal RLVs are unity in our dimensionless units so ($q = 1/\sqrt{3}$). The parameters A_s and B_s are solved by substituting Eq. (27) into Eqs. (19) and (20) and by minimizing the resulting free-energy F with respect to A_s and B_s. This minimization yields the solid free energy density

$$\begin{aligned}f_s(\bar{\psi}_s) &= 4\,(-\epsilon + 3\bar{\psi}_s^2)A_s^2 + 3\,(-\epsilon + 3\bar{\psi}_s^2 + \frac{R_1}{9})B_s^2 \\ &\quad +72\bar{\psi}_s A_s^2 B_s + 144A_s^2B_s^2 + 54A_s^4 + \frac{45}{2}B_s^4 \\ &\quad -\frac{\epsilon}{2}\bar{\psi}_s^2 + \frac{R_1}{2}\bar{\psi}_s^2 + \frac{8}{9}\bar{\psi}_s^2 + \frac{1}{4}\bar{\psi}_s^4, \qquad (28)\end{aligned}$$

where A_s and B_s are themselves functions of $\bar{\psi}$. The coexistence densities $\bar{\psi}_s$ and $\bar{\psi}_l$ are computed numerically using the standard common tangent construction, which consists of equating the chemical potentials $f_s'(\bar{\psi}_s) = f_l'(\bar{\psi}_l) = \mu_E$ and grand potentials $f_s(\bar{\psi}_s) - \mu_E\bar{\psi}_s = f_l(\bar{\psi}_l) - \mu_E\bar{\psi}_l$ of the two phases. It is also necessary to compute the solid free-energy curve for bcc since the latter can have a lower free-energy than fcc for some regions of the phase diagram. The bcc free-energy density was obtained by expanding the crystal density field using a one-mode approximation, which only involves $\langle 110\rangle$ RLVs as in Ref. [14], and substituting this expansion into the two-mode model defined by Eqs. (19) and (20).

An example of the phase diagram for $R_1 = 0.05$ is shown in Fig. 1, where we also show for completeness the hexagonal and stripe phases. As desired, we obtain a large ϵ range of fcc-liquid coexistence. For small ϵ, however, bcc becomes favored over fcc. A common tangent construction using fcc and bcc free-energy curves shows that the density range of bcc-fcc coexistence is extremely narrow for small values of ϵ and cannot be resolved on the scale of Fig. 1. As will be explained later in section III C, the range of ϵ where bcc is favored depends on the value of R_1. In the limit $R_1 \gg 1$, the two-mode model reduces to the standard one-mode model after a simple rescaling of parameters, which can be easily seen by comparing Eqs. (20) and (25). Hence, increasing R_1 reduces the contribution of the second mode. Conversely, reducing R_1 increases the contribution of this mode and tends to favor the fcc structure, which extends to smaller ϵ for smaller R_1. In the extreme case where $R_1 = 0$, the region of fcc-liquid coexistence extends all the way to vanishingly small ϵ as shown in Fig. 2.